MODELLING THE IMPACT OF TRANSPORT PROCESSES ON OZONE WITH GEM-MARS: A COMPARISON WITH MARCI.

L. Neary, F. Daerden, *Belgian Institute for Space Aeronomy, Brussels, Belgium*, **R. T. Clancy, M. J. Wolff,** *Space Science Institute, Boulder, Colorado, USA*.

Introduction

The composition of the Martian atmosphere is driven by a complex system of photochemistry, transport and small scale processes. Global Circulation Models (GCMs) are a crucial tool in the interpretation of observations, as has recently been shown by Clancy et al. (2012, 2013a), Bertaux et al. (2012), Federova et al. (2012) and Montmessin and Lefèvre (2013) for example. In anticipation of the ExoMars Trace Gas Orbiter (TGO) mission, the GEM-Mars model is used to analyse the photochemistry of the Martian atmosphere. Comparisons are made with recent observations from the Mars Color Imager (MARCI) on the Mars Reconnaissance Orbiter (MRO) (Malin et al., 2001, Clancy et al., 2013) with some discussion regarding mixing in the free atmosphere and transport processes.

Gas-phase chemistry

The chemical package included online in GEM-Mars uses reactions and rate coefficients based on the work of Garcìa-Muñoz et al. (2005). There are 15 photolysis and 31 chemical reactions (solved implicitly using Gaussian elimination method) and include the following 13 species: O_3, O_2, $O(^1D)$, O, CO, H, H_2, OH, HO_2, H_2O, H_2O_2, $O_2(a^1\Delta_g)$ and CO_2.

The chemical species are transported and mixed by the resolved circulation, eddy diffusion and in the upper atmosphere, molecular diffusion. Other physical parameterisations included in the model are a 14 layer soil model with sub-surface ice, CO_2 condensation/sublimation and a water cycle with simple bulk condensation. The simulations presented are made with horizontal resolution 4°x4°, 103 staggered vertical levels up to approximately 160 km, and a 30 minute timestep.

In the chemical scheme, ozone is produced by the following reaction:

$$O + O_2 + CO_2 \rightarrow O_3 + CO_2$$

and is destroyed by photolysis, reactions with $O(^1D)$ and most importantly, several reactions involving the products of H_2O dissociation. Therefore, it is crucial to represent the water cycle correctly in the model as it is the driver for ozone. A comparison of GEM-Mars water vapour column with observations from the Thermal Emission Spectrometer (TES) (Smith, 2002) at 3 latitude bands is given in Figure 1. For the first half of the year, the model compares well with the timing and magnitude of the water column, although the model slightly under-predicts at 60°N. The second half of the year is during the dust storm season and the model over-predicts the column amounts by about 5 pr-μm. This version of GEM-Mars uses a prescribed dust scenario with a Conrath profile shape which leads to warmer temperatures in the northern hemisphere during this time.

Transport also plays a role in the distribution of ozone as shown in Montmessin and Lefèvre (2013). Figure 2 shows the zonal mean vertical distribution of ozone at L_s 90° from the model. A distinct layer can be seen at 60 km in the southern polar region which is a result of air containing extra oxygen being transported from lower latitudes to the polar night.

Comparison with MARCI

In Figure 3, the comparison of the zonally averaged daytime column ozone from GEM-Mars and MARCI shows that the overall pattern is represented by the model. The maximums seen at high latitudes in fall, winter and spring are reproduced, but the mid-latitude values are slightly higher than observed. In the northern hemisphere spring between L_s 30-60° the MARCI data shows high column amounts around 60-70°N. This maximum is not seen to be as strong in the model values. This may be a result of heterogeneous chemistry (not included in this version of the model) where HO_x radical species react on the surface of ice particles, leading to less ozone destruction (as described in Lefèvre et al., 2008).

Model sensitivity studies showed that the free atmosphere stability functions and mixing length used can have a significant impact on the ozone column amount in the polar spring and summer. In the polar night within the vortex, there is very little mixing. In spring, around 60-70N latitude, planetary wave structures produce strong variability at a given point, where air from inside and outside the vortex pass over (see Figure 4). If there is little contrast in the mixing length inside and outside the vortex, the variability seen in the model is much lower. When the mixing length is lowered inside the vortex, the comparison is better, although still low (as expected, given the horizontal resolution of the simulations). This is shown in Figure 5 with a time series of the ozone column from L_s 0 to 26 at 70-74N latitude. The model values are coloured by the ice optical depth to indicate that heterogeneous chemistry may also play

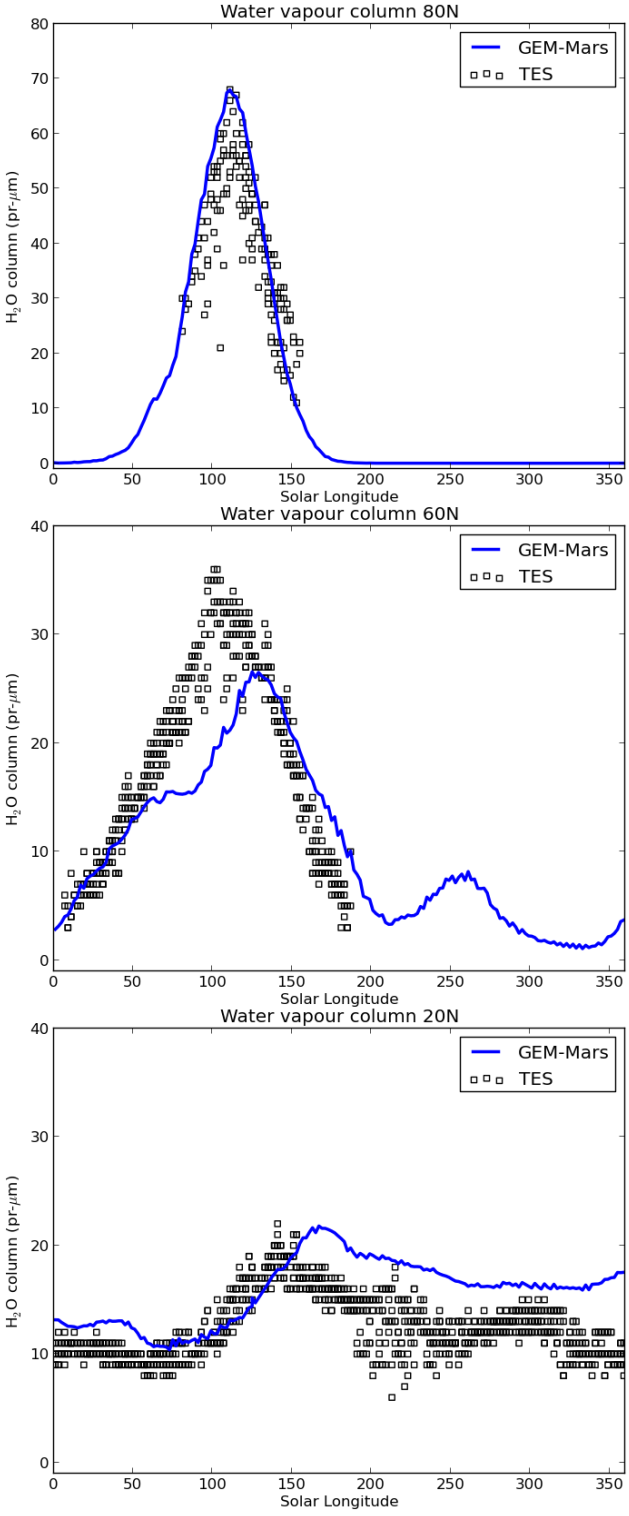

Figure 1: GEM-Mars water vapour column at 80N (top), 60N (centre) and 20N (bottom).

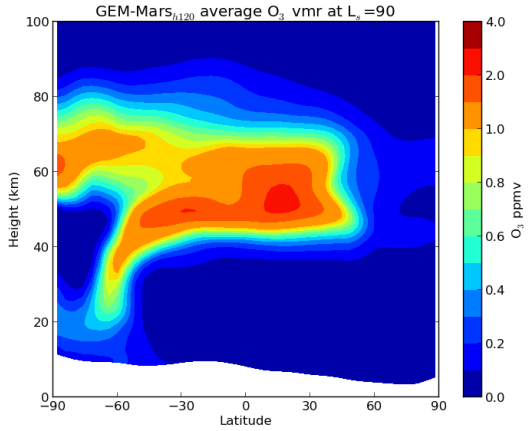

Figure 2: GEM-Mars zonal mean profile of ozone at L_s=90.

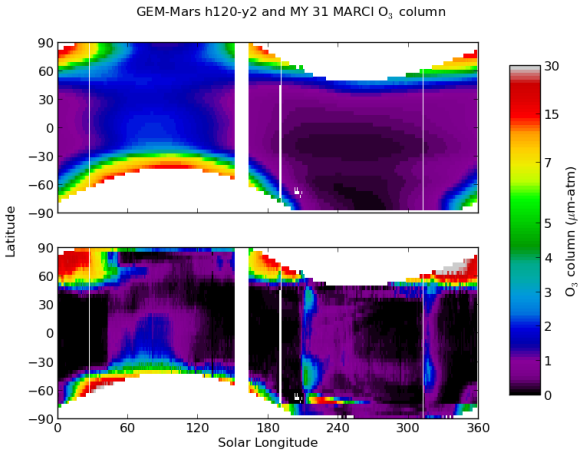

Figure 3: Comparison of GEM-Mars (top) and MARCI (bottom) zonal mean daytime column ozone.

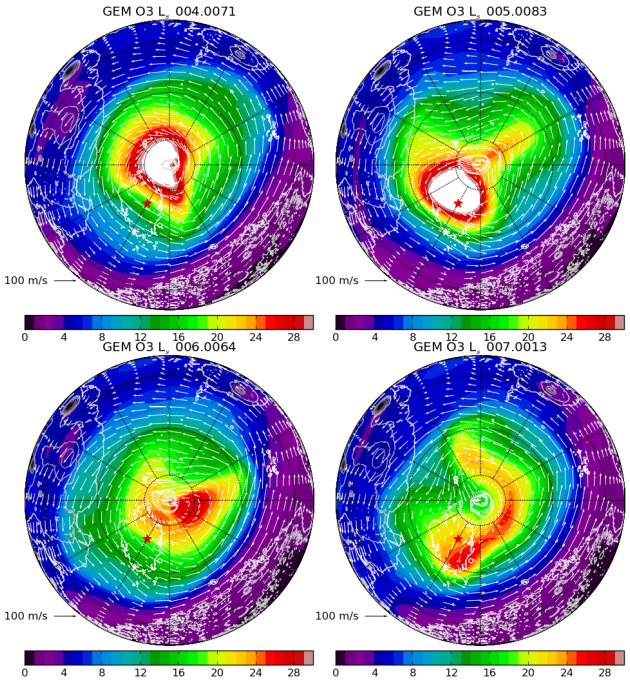

Figure 4: GEM-Mars north polar snapshots of column ozone with wind field at ∼25km at 4 times (L_s 4-7°). The red star is just to indicate one point for reference.

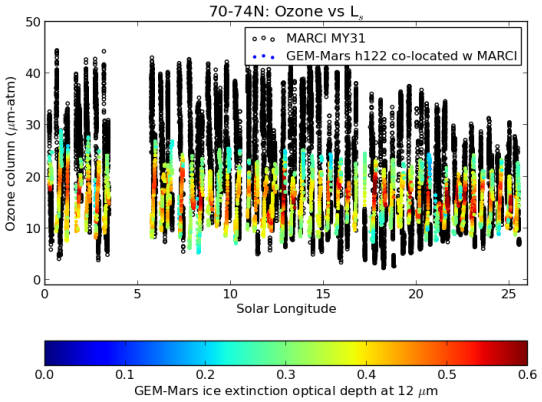

Figure 5: Time series from L_s=0-26° at 70-74°N latitude of ozone column as measured by MARCI (black circles) and simulated by GEM-Mars (markers coloured by GEM-Mars water ice extinction optical depth).

a role here.

As summer arrives, water vapour released from the polar cap is mixed upwards (and the HO_x products of H_2O photolysis), destroying ozone in the upper layer. If the free atmosphere mixing is too low, the water remains in the lower atmosphere and the decrease in column ozone is less (see Figure 6). The total column amount of water vapour does not change significantly, but it is the vertical distribution that is important in this case.

Discussion and conclusions

The GEM-Mars model is able to reproduce the basic features seen in the observations of ozone made by the MARCI instrument. In the north polar summer, when the water ice cap sublimates, mixing in the free atmosphere plays a role in the vertical distribution of water vapour and therefore the column amount of ozone.

Some processes are not included in the model version used for these results, including hetergeneous chemistry, non-condensible gas-enrichment and interactive dust and clouds. The implementation of these processes is currently underway.

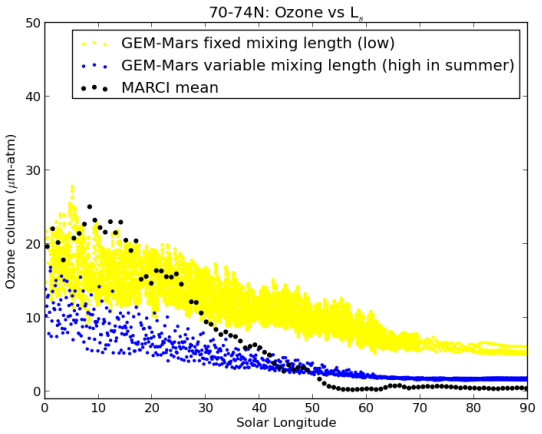

Figure 6: Time series from L_s=0-90° at 70-74°N latitude of ozone column as measured by MARCI (black circles) and simulated by GEM-Mars with different mixing lengths.

References

[1] Bertaux, J.L., Gondet, B., Lefèvre, F., Bibring, J.P., and Montmessin, F. (2012). First detection of O_2 1.27 μm nightglow emission at Mars with OMEGA/MEX and comparison with general circulation model predictions. Journal of Geophysical Research 117.

[2] Clancy, R.T., Sandor, B.J., Wolff, M.J., Smith, M.D., Lefèvre, F., Madeleine, J.-B., Forget, F., Murchie, S.L., Seelos, F.P., Seelos, K.D., et al. (2012). Extensive MRO CRISM observations of 1.27 μm O2 airglow in Mars polar night and their comparison to MRO MCS temperature profiles and LMD GCM simulations. Journal of Geophysical Research: Planets 117.

[3] Clancy, R. T., Sandor, B.J., García-Muñoz, A., Lefèvre, F., Smith, M.D., Wolff, M.J., Montmessin, F., Murchie, S.L., and Nair, H. (2013a). First detection of Mars atmospheric hydroxyl: CRISM Near-IR measurement versus LMD GCM simulation of OH Meinel band emission in the Mars polar winter atmosphere. Icarus 226, 272.

[4] Clancy, R.T., M. J. Wolff, F. Lefèvre, M. Malin, (2013b). The full seasonal/global variations of Mars ozone from MARCI 2006-2013 daily global mapping retrievals, Bull. Amer. Astron. Soc, v45, p 164.

[5] Fedorova, A.A., Lefèvre, F., Guslyakova, S., Korablev, O., Bertaux, J.-L., Montmessin, F., Reberac, A., and Gondet, B. (2012). The O_2 nightglow in the martian atmosphere by SPICAM onboard of Mars-Express. Icarus 219.

[6] García-Muñoz, A., McConnell, J.C., McDade, I.C., and Melo, S.M.L. (2005). Airglow on Mars: Some model expectations for the OH Meinel bands and the O_2 IR atmospheric band. Icarus 176, 75-95.

[7] Lefvre, F., Bertaux, J.-L., Clancy, R.T., Encrenaz, T., Fast, K., Forget, F., Lebonnois, S., Montmessin, F., and Perrier, S. (2008). Heterogeneous chemistry in the atmosphere of Mars. Nature 454, 971975.

[8] Malin, M.C., Bell, J.F., Calvin, W., Clancy, R.T., Haberle, R.M., James, P.B., Lee, S.W., Thomas, P.C., and Caplinger, M.A. (2001). Mars Color Imager (MARCI) on the Mars Climate Orbiter. Journal of Geophysical Research: Planets 106.

[9] Montmessin, F., and Lefèvre, F. (2013). Transport-driven formation of a polar ozone layer on Mars. Nature Geoscience.

[10] Smith, M.D. (2002). The annual cycle of water vapor on Mars as observed by the Thermal Emission Spectrometer. Journal of Geophysical Research 107.